H. NISHIOKA[✉]

K.-I. UEDA

Super-broadband continuum generation with transient self-focusing of a terawatt laser pulse in rare gases

Institute for Laser Science, University of Electro-Communications, 1-5-1 Chofugaoka, Chofu, Tokyo 182-8585, Japan

ABSTRACT Hyper-continuum that continuously covers from the VUV to the IR spectral regions with a flat spectral shape has been generated in nonlinear propagation in rare gases. The spectral intensity was 1 GW/nm with a conversion efficiency of > 50%. The spectral, spatial, and temporal characteristics have been studied.

PACS 42.65.Jx; 42.65.Re

1   Introduction

Since spectral broadening by a pulsed laser was observed in a Q-switched laser pulse in 1967 [1], frequency extension based on nonlinear phase modulation has been intensively studied [2]. In the early stage, because of limited laser intensity, solid and liquid nonlinear materials that have a large nonlinear refractive index due to their resonant absorption in the UV or blue region were used. Therefore, the bandwidth of the super-continuum generated in the condensed media is essentially limited within the VIS or IR region. After the invention of the chirped pulse amplification [3] scheme, the peak intensity of ultra-short pulses has drastically increased. Terawatt to sub-petawatt [4] laser power can now be generated in a tabletop system with high repetition rate. The high peak power effectively induces a nonlinear refractive index even in low-density and/or highly transmitting media. Especially, rare gases [5, 6] are entirely transparent in the light-wavelength regions with perfect photochemical stabilities. The nonlinear frequency broadening in rare gases is efficient to generate very short wavelength, high peak power, and high average power radiation. Intense super-broadband radiation has been generated in the VUV-IR (150–900 nm) region [7]. Following this, continuously tunable second-harmonic frequency conversion from the mid-IR continuum to the VIS [8, 9] has demonstrated the existence of intense continuum at longer wavelengths. Recently, spectroscopic measurements in the mid-IR [10] and sub-THz regions [11] were reported. Backward scattering in the self-trapped filament created in air was studied [12] for lidar applications. Alternatively, white light generated in rare gas [7] has

been used to increase UV spectral intensities in these applications [13]. In the time domain, the intense radiation having an ultra-short pulse width and a coherent time is efficient for super-fast nonlinear optics [14].

In this paper, we introduce an ultra-broadband and efficient frequency-conversion technique based on both spatial and temporal self-phase modulations (SPMs) in rare gases.

2   Frequency broadening in transient self-trapping

2.1   *Self-trapping condition*

As well known as the self-focusing, the index of refraction is a function of light intensity. The self-focusing is spatial self-phase modulation. Assuming that $n_2 > 0$, a nonlinear medium placed at the center of a laser beam where the light intensity is higher than at a peripheral region forms a convex lens. The phase delay due to the nonlinear refractive index n_2 is given by the B-integral factor, $B = (2\pi/\lambda) \int_0^L n_2 I_L \mathrm{d}z$, where I_L, λ, and L are laser intensity, laser wavelength, and interaction length, respectively. On the other hand, diffraction through the beam waist shows a positive phase shift (the Guoy phase shift). The axial phase shift φ due to the diffraction is given by $\varphi = \tan^{-1}(z/z_R) \cong z/z_R$, where $z_R = \pi w_0^2/\lambda$ is the Rayleigh range with beam waist w_0. At $z = z_R$, the phase shift is $\varphi = \pi/4$. When $B > \varphi$ through z_R, the beam will converge to a small spot. If a critical balancing condition $\varphi(z = z_R) = B(z = z_R) = \pi/4$ is satisfied, the laser pulse propagates in the nonlinear medium with a constant beam-waist size $w_{0,\mathrm{st}} = \lambda (8\pi n_2 I_L)^{1/2}$ because both B and φ are the same function of beam radius, i.e. they are proportional to w_0^{-2} when we assume that the laser power is kept constant. The balancing condition is independent of the beam-waist size of the self-trapping $w_{0,\mathrm{st}}$ or I_L, but it is satisfied only at the critical power of self-trapping $p_{0,\mathrm{st}} = \pi w_{0,\mathrm{st}}^2 I_L = \lambda^2/8n_2$. For example, in air ($n_2 = 8.2 \times 10^{-2}\,\mathrm{W/cm^2}$) at $\lambda = 800\,\mathrm{nm}$, $p_{0,\mathrm{st}} = 10\,\mathrm{GW}$. This theoretical explanation without a plasma contribution to the defocusing well agrees with the measurements reported. The whole-beam self-focusing data shows a critical power of 10 GW (2 mJ for a 200-fs pulse [15]).

Some theoretical analysis [16, 17] reported that high-density plasma generated in the propagating channel is the main contributor for the negative refractive index, instead of the diffraction discussed above. The calculations assume an electron density of 1–$5 \times 10^{16}\,\mathrm{cm^{-3}}$ in the channel.

[✉] Fax: +81-424/85-8960, E-mail: nishioka@ils.uec.ac.jp

Filling a channel in air having a diameter of $100\,\mu$m and a length of 10 m with electrons having the number density of $5 \times 10^{16}\,cm^{-3}$, a laser energy of 10 mJ must be absorbed during propagation. The energy loss of 10 mJ per channel is, however, five times higher than the initial laser energy of the self-trapping experiments. Our measurements show that the trapped laser pulse after 10-m propagation in air still has more than 90% of the initial energy. Thus the plasma density should be, at least, one order lower than the theoretically estimated value based on plasma defocusing [18].

When the initial laser power exceeds the critical power, the self-focusing increases the laser intensity and then non-linear absorption appears. The nonlinear absorption possibly plays a role of an intensity limiter at an early stage of the self-trapping. The maximum intensity limited by the nonlinear absorption is typically in the order of 10^{13-14} W/cm^2 [7]. Owing to the moderate energy loss due to the nonlinear absorption, the total laser power approaches the critical power and so finally the self-focusing balances the diffraction. Once this condition is established the laser intensity is kept constant at slightly below the ionization threshold. Thus, the absorption loss in the following propagation is negligible.

2.2   Pulse shaping due to the self-trapping

The self-focusing is electronic; its response time is shorter than a femtosecond laser pulse width. The self-trapping occur only in a limited duration when the instantaneous laser power exceeds the critical power $p(t) \geq p_{0,st}$. The peak intensity of a trapped laser pulse continuously increases up to the ionization threshold of the medium. In contrast, the former and tail parts of the pulse lose intensity down to a negligibly small value because diffraction is effective below the threshold. This physical picture is called a 'moving focus' or a 'laser bullet'. The pulse duration of the trapped laser pulse is effectively shortened by the spatial modulation, i.e. a 'Kerr-lens filter effect'.

2.3   Self-phase modulation and optical parametric effect in/between self-trapping channels

The self-trapping discussed is a part of the phase modulation in the space domain. On the other hand, in the time domain, the phase modulation extends the spectrum of the laser radiation. Both the spatial and the temporal self-phase modulations are due to the same nonlinear refractive index. The self-trapped laser pulse has a high intensity and a short duration. These conditions effectively induce SPM (in time) in gas media because frequency extension due to the SPM is proportional to $-dI_L(t)/dt$. Further frequency extension can be expected with multi-photon pumped optical parametric processes.

For example, the optical parametric amplification with $\chi^{(3)}$ susceptibility divides a pair of pump photons into a pair of signal and idler photons. If the nonlinear medium has a high transmittance for both the signal and idler wavelengths (i.e. rare gases), the frequency conversion is very efficient. In addition, group-delay dispersion (GDD) mismatch between the signal and idler is insignificant in the low-dispersive media. The phase-matching condition of four-wave mixing can be satisfied for an ultra-broad spectral bandwidth when two
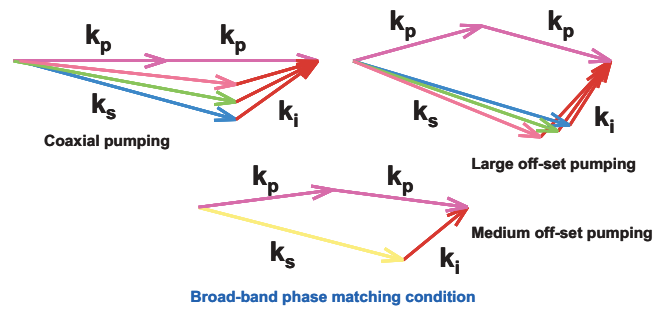

FIGURE 1   condition in a two photon pumped optical parametric amplifier using non-collinear pumping. The vectors, k_p, k_s, and k_i, are the pump, signal, and idler wave vectors, respectively

pump photons are located in the off-axis geometry [19, 20] as shown in Fig. 1. The optimum angle between the two pump beams depends on the dispersion of the medium. The angle is quite small in atmospheric pressure gas media (a few mrad) so that the off-axis phase matching is easily satisfied with a single pump beam if the pump beam has a small divergent or convergent angle.

3   Continuum generation with multi-channel propagation of self-trapped terawatt laser pulses in gas media

3.1   Experimental setup for multi-channel propagation

A 2-terawatt (TW) Ti:Al$_2$O$_3$ laser system producing 250 mJ with 120-fs pulse duration was used. The 2-TW laser output in a beam diameter of 4 cm corresponds to an intensity of 160 GW/cm^2. The laser intensity far exceeds the critical power of the self-trapping [21]. The self-trapping appeared 10 m from the compressor and propagated the remaining 20 m of the corridor. We introduce multi-channel propagation of the self-trapped laser pulse to satisfy the off-axis ultra-broad phase-matching condition of the multi-photon pumped optical parametric amplifier (OPA). To form the off-axis multi-channel propagation, a focusing lens of $f = 5$ m was used. The laser beam forms multi-channel self-trapped beams behind its focal point. Beam profiles of the multi-channel propagation 5 m behind the focus are shown in Fig. 2 with various laser powers. At the threshold power of the self-trapping, a single beam is observed at the center of the beam cone. The number of the channels rapidly increases with laser power. Over 1 TW, the beam cone is closely filled with a large number of the self-trapped filaments. Adjacent filaments having a small angle to each other satisfy the off-axis ultra-broadband phase-matching condition. Strong white radiation, the hyper-continuum (HC), has been observed above the threshold of self-trapping. As shown as peripherals in Fig. 2, super-continuum generated in solid-state media shows a white beam core (the SPM) surrounded by colored rings. The latter have a large cone angle far exceeding that of the pump beam. The large cone angle is due to large dispersion in the condensed media under the phase-matching condition of the two-photon pumped OPA.
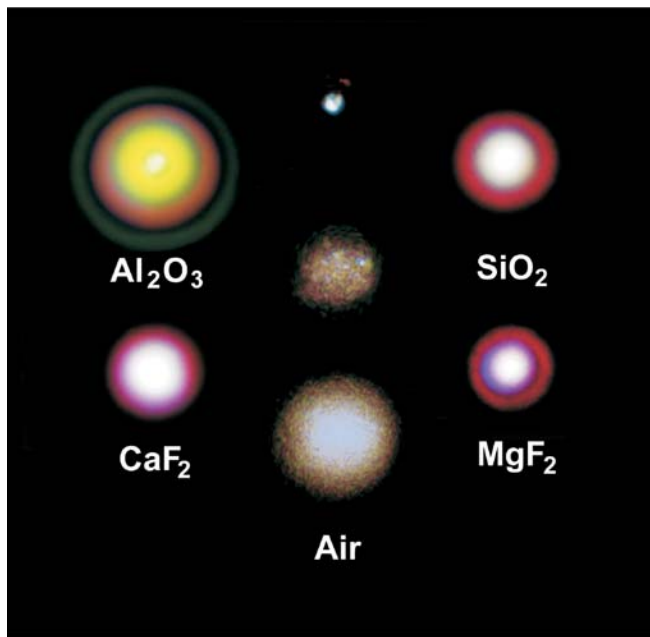
FIGURE 2   The beam profiles of the self-trapped lasers pulse in air, at the laser power of 0.17 TW (*center-upper*), 0.52 TW (*center-mid.*) and 1.6 TW (*center-lower*). These pictures are taken 5 m from the focus of $f = 5$ m lens. The surrounding colorful pictures are conventional supercontinuum generated in solid-state materials. (These were taken approximately 0.3 m from the focus)

FIGURE 4   Spectral intensities under the multi-channel propagation in atmospheric pressure xenon as a function of laser power. The pump laser pulse width is 120 fs

3.2   *Spectral properties of the hyper-continuum*

The spectral intensity of the HC obtained in atmospheric pressure rare gases was 1 GW/nm in the UV to VIS region as shown in Fig. 3. In these measurements, the pump beam was focused into a 9-m-length gas cell with a $f = 5$ m lens. The focal point was placed 3 m from the input window. The two spectral peaks in Ar in the VUV region correspond to the 5th and 7th harmonics of the 790-nm laser pulse, respectively. The cut-off wavelength of 150 nm is very close to the 5th harmonic. The bandwidth of the upper side band

(from the laser frequency to the VUV cut-off) was 1.6 PHz, corresponding to four times the laser carrier frequency. The energy-conversion efficiency from the pump laser to the side band has been measured to be 50% in Ar by eliminating the pump laser spectrum (> 740 nm) with a dichroic mirror. Spectral intensities obtained in xenon as a function of the laser power are shown in Fig. 4. The ultra-broadband and flat spectrum shape was observed above the threshold of self-trapping. As the pump power increases, the spectral intensity grows super-linearly. Because xenon has the highest nonlinear refractive index and the lowest ionization energy in rare gases, the multi-photon absorption limits the growth rate of the UV spectral intensity. Thus, xenon shows the highest spectral intensity in the VIS-IR and mid-IR regions (as shown in Fig. 5) but the cut-off wavelength in the VUV is the longest.

The SPM followed by the OPA quickly broaden the spectral width to the UV region. The comparison of the spectral intensity between 6-m and 9-m gas cells is shown in Fig. 6. In both cells, the focus of the $f = 5$ m lens was located 3 m from the input window, so the effective interaction lengths in these cells were 3 m and 6 m, respectively. The spectral shapes are almost the same but the conversion efficiency growths with the interaction length.
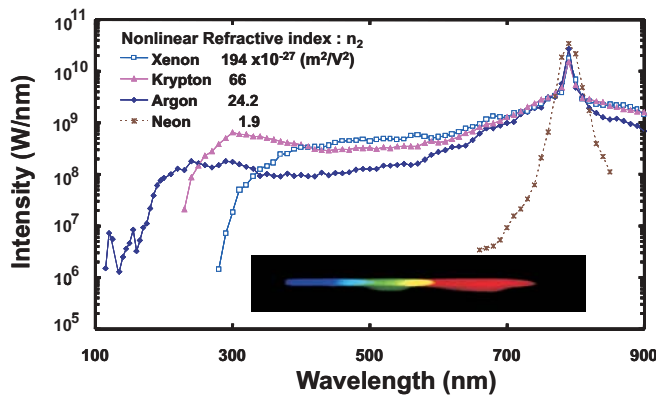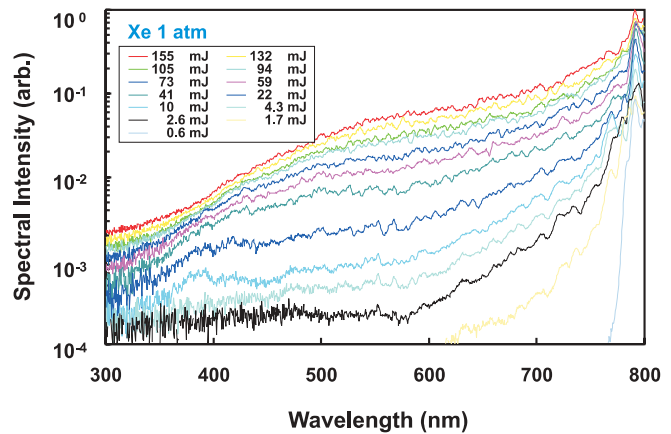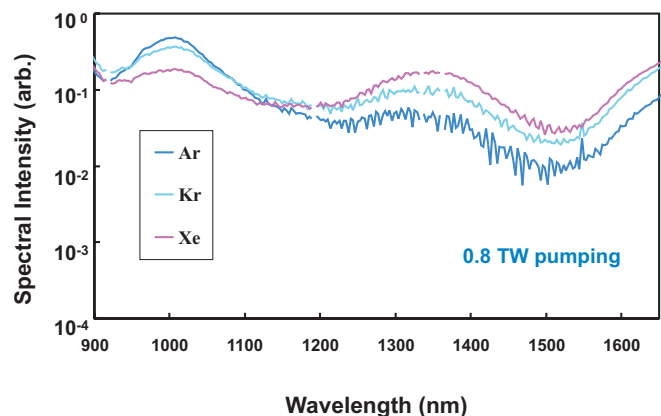

FIGURE 3   Spectral intensities of the hypercontinuum generated in atmospheric pressure rare gases. The pump laser wavelength and power are 790 nm and 1.6 TW, respectively. The two small peaks appeared in the VUV region corresponding to the 5th and 7th harmonics, respectively. The spectrum obtained in neon is showing typical spectrum shape due to non-trapped self-phase-modulation

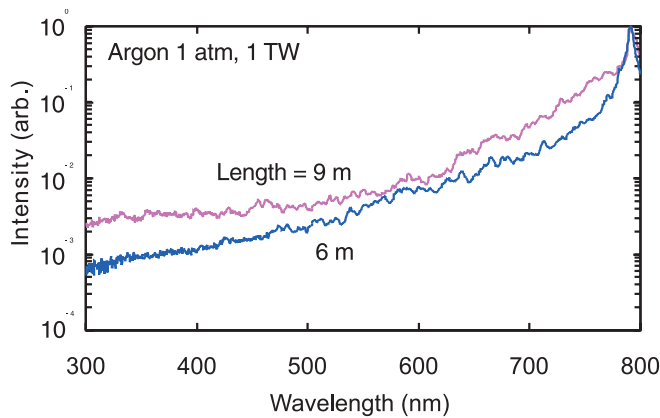FIGURE 5   Spectral intensities in the mid-IR region in rare gases

FIGURE 6 Comparison of the spectral intensity between the 6 m and 9 m length gas cells. The interaction lengths behind focus for these cells are 3 m and 6 m, respectively

3.3 *Far-field beam profile and group-delay dispersion of the self-trapped laser pulse*

The far-field beam profile of the HC measured with the knife-edge scanning method is shown in Fig. 7. The beam profiles were measured by eliminating spectrum components near the pump laser wavelength (longer than 740 nm) using a dichroic mirror. In Kr, significant spatial modulation due to the self-trapping was observed. The beam divergence in Ar was measured to be 0.9 mrad, which is smaller than that of the pump beam. The improvement in spatial beam quality is due to whole-beam self-focusing that plays a role as an active spatial filter. The whole-beam self-focusing decreases its waist size without reduction of the laser power.

The pulse width and group-delay dispersion have been measured with a cross-correlation technique [22]. A spectral component of the HC was mixed with the 790-nm pump laser pulse having the pulse duration of 120 fs. The second-order cross-correlation function is shown in Fig. 8. The pulse duration of the spectral components with a limited spectra width of 30 nm has been measured to be 150–250 fs assuming a sech^2 pulse shape. Between the spectral components of 615 nm and 1110 nm, a group delay of 500 fs was observed as shown in Fig. 9. The group-delay dis-
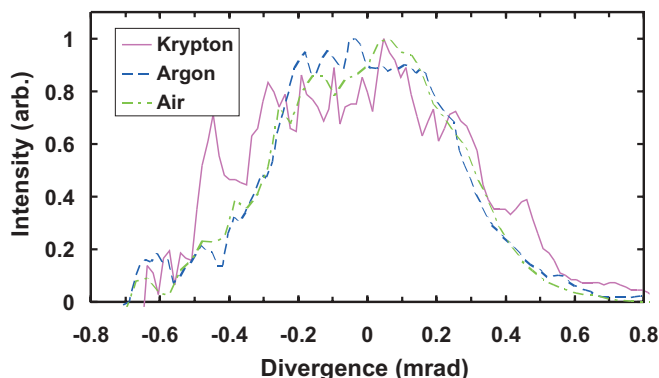

FIGURE 7 Far-field beam profile of the hyper-continua generated in atmospheric pressure gasses
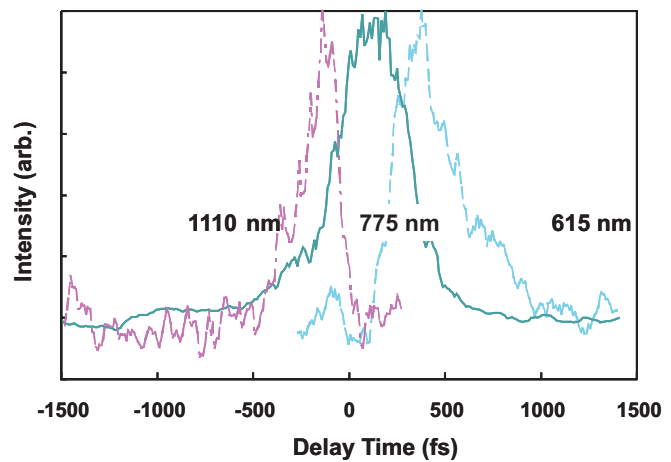

FIGURE 8 Cross-correlation trace of the HC generated in Kr. The origin of the delay time is taken at an arrival time of the 790 nm pump laser pulse
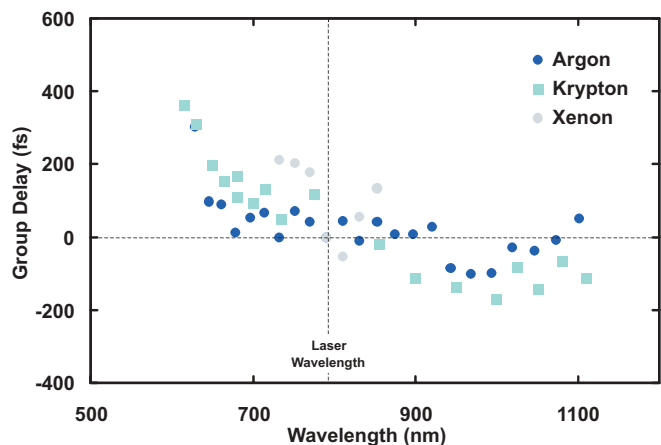

FIGURE 9 Group delay dispersion in atmospheric pressure rare gases

persion of $\frac{\Delta t}{\Delta \lambda} = 1$ fs/nm is significantly smaller than the super-continuum generated in a solid-state or liquid medium. The small GDD has an advantage in the pulse compression using a low negative dispersion but precisely controlling devices such as chirped mirrors or spatial phase modulators [23].

4 Application for super-broadband and super-fast measurements

The HC, coherent broadband and intense radiation, has feasibilities for high-speed pumping and monitoring experiments. The HC can excite multiple absorption bands simultaneously and then material coherences [24] will be excited. For example, we have demonstrated coherence control in a multi-level system having an ultra-fast dephasing time ($T_2 \approx 15$ fs). By changing an interaction phase between the excited coherences and the broadband light field, amplitude and phase of the coherence have been controlled. A symmetric and coaxial two-pulse pumping system having a monocycle temporal resolution of 1.4 fs was used to control coherences in a λ-type three-level system in a dye solution [14]. The interference between two excited coherences has been observed in the absorption as shown in Fig. 10. The two saturation peaks appeared at 5.1 fs under the strongly coupled
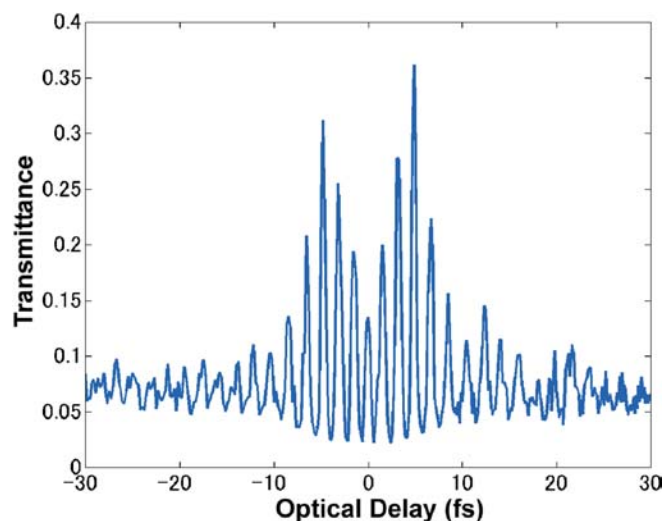
FIGURE 10 Phase-resolved absorption saturation in Rh6G dye solution as a function of optical delay between two-pump pulses. Two peaks (absorption saturation at 5.1 fs) were observed when Rabi frequency exceeds absorption bandwidth: $\omega_R > \omega_a = 30\,\text{THz}$

condition, i.e. the Rabi frequency ω_R exceeds the absorption and emission line width ω_a. The separation of the two peaks was 5–6 optical cycles. This fast response shorter than the natural dephasing time of 15 fs clearly shows the coupling of the excited coherences. The trace shown in Fig. 10 was measured with a repetition rate of 10 Hz. The stability of the HC was sufficient for high-speed and nonlinear pump–probe measurements.

5   Summary

It has been demonstrated that efficient frequency extending to the VUV region from a femtosecond IR laser pulse is possible in atmospheric pressure rare gases with the noncollinear multi-channel self-trapping geometry. The bandwidth of 1.6 PHz corresponding to a coherence time of 0.2 fs was used to demonstrate the ultra-fast multi-frequency nonlinear optics with monocycle pumping and probing temporal resolutions.

REFERENCES

1 F. Shimizu: Phys. Rev. Lett. **19**, 1097 (1967)
2 R.R. Alfano (Ed.): *The Supercontinuum Laser Source* (Springer, Berlin 1989)
3 D. Strickland, G. Mourou: Opt. Commun. **56**, 219 (1985)
4 K. Yamakawa, M. Aoyama, S. Matsuoka, T. Kase, Y. Akahane, H. Takuma: Opt. Lett. **23**, 1468 (1998)
5 P.B. Corkum, P.P. Ho, R.R. Alfano, J.T. Manassah: Opt. Lett. **10**, 624 (1985)
6 Y. Shimoji, A.T. Fay, R.S.F. Chang, N. Djeu: J. Opt. Soc. Am. B **6**, 1994 (1989)
7 H. Nishioka, W. Odajima, K. Ueda, H. Takuma: Opt. Lett. **20**, 2505 (1995)
8 H. Nishioka, W. Odajima, M. Tateno, K. Ueda, A.A. Kaminskii, A.V. Butashin, S.N. Bagayev, A.A. Pavlyuk: Appl. Phys Lett. **70**, 1366 (1997)
9 A.A. Kaminskii, A. Butashin, H. Eichler, D. Grebe, R. Macdonald, K. Ueda, H. Nishioka, W. Odajima, M. Tateno, J. Song, M. Musha, S. Bagayev, A. Pavlyuk: Opt. Mater. **7**, 59 (1997)
10 J. Kasparian, R. Sauerbrey, D. Mondelain, S. Niedermeier, J. Yu, J.-P. Wolf, Y.-B. Andre, M. France, B. Prade, S. Tzortzakis, A. Mysyrowicz, M. Rodriguez, H. Wille, L. Woste: Opt. Lett. **25**, 1397 (2000)
11 S. Tzortzakis, G. Mechain, G. Ptalano, Y.-B. Andre, B. Prade, M. Franco, A. Mysyrowicz, J.-M. Munier, M. Gheudin, G. Beaudin, P. Encrenaz: Opt. Lett. **27**, 1944 (2002)
12 J. Yu, D. Mondelain, G. Ange, R. Volk, S. Niedermeier, J.P. Wolf, J. Kasparian, R. Sauerbrey: Opt. Lett. **26**, 533 (2001)
13 M.C. Galvez, M. Fujita, N. Inoue, R. Moriki, Y. Izawa, C. Yamanaka: Jpn. J. Appl. Phys. **41**, L284 (2002)
14 H. Nishioka, K. Ueda: Appl. Phys. B **74**, S89 (2002)
15 A. Braun, G. Korn, X. Liu, D. Du, J. Squier, G. Mourou: Opt. Lett. **20**, 73 (1995)
16 E.T.J. Nibbering, P.F. Curley, G. Grillon, B.S. Prade, M.A. Franco, F. Salin, A. Mysyrowier: Opt. Lett. **21**, 62 (1996)
17 H.R. Lange, G. Grillon, J.-F. Ripoche, M.A. Franco, B. Lamouroux, B.S. Prade, A. Mysyroxicz, E.T.J. Nibbering, A. Chiron: Opt. Lett. **23**, 120 (1998)
18 M. Nurhuda, A. Suda, K. Midorikawa: RIKEN Rev. **48**, 40 (2002)
19 H. Nishioka, K. Ueda: in Proc. 16th Int. Conf. Coherent and Nonlinear Optics '98, SPIE **3734**, 10 (1998)
20 H. Nishioka: in Proc. US–Japan Semin. Manipulation of Matter by Coherent Light, Kusatsu Gunma, Japan, 1–5 September 1997
21 H. Nishioka, W. Odajime, K. Ueda: in Proc. 11th Int. Conf. Vacuum Ultraviolet Radiation Physics, Spec. Iss. J. Electron Spectrosc. Relat. Phenom. **80**, 263 (1996)
22 H. Nishioka, W. Odajima, Y. Sasaki, K. Ueda: Prog. Cryst. Growth Character. Mater. **33**, 237 (1996)
23 L. Xu, Liming Li, N. Nakagawa, R. Morita, M. Yamashita: IEEE Photon. Technol. Lett. **12**, 1540 (2000)
24 U. Fano: Phys. Rev. **124**, 1866 (1961)